Tom Doman for computational assistance, to Dr. Sergio Deganello and Prof. Robert Bau for assistance with the calculations of internuclear distances, to Giulia Gulia for a sample of $[IrH_5(PPr^i_3)_2]$, and to Johnson Matthey for a generous loan of osmium.

Appendix: Calculation of the Hydride Relaxation Rate in $[ReH_5(PMePh_2)_3]$

Using the unit cell parameters and fractional atomic coordinates determined by neutron diffraction,[9a] the internuclear distances, r_{HX}, between each of the five hydrides and all other dipolar nuclei, including other hydrides, ortho hydrogens, methyl hydrogens, phosphorus, and rhenium nuclei in $[ReH_5(PMePh_2)_3]$ were calculated by means of eq 19, where a, b, c, α, β, and γ are the unit

$$r_{HX} = \{(a\Delta x)^2 + (b\Delta y)^2 + (c\Delta z)^2 + 2ab\Delta x\Delta y \cos\gamma + 2ac\Delta x\Delta z \cos\beta + 2bc\Delta y\Delta z \cos\alpha\}^{0.5} \quad (19)$$

cell parameters and Δx, Δy, and Δz are the differences between the fractional atomic coordinates of the two nuclei (Table X). (Meta and para proton are neglected because their contributions to the hydride relaxation rate are negligible.)

Contributions to the relaxation rates from the individual dipole–dipole interactions were calculated as follows. For proton–proton interactions, the relaxation rate is calculated by using eq 4, where r_{HH} is the internuclear distance between the two protons (Å). The sum of the relaxation rates for interaction of hydride

$$R_{HH} = \frac{77.51\ \text{Å}^6\ \text{s}^{-1}}{(r_{HH})^6} \quad (4)$$

HT11 with each of the four other hydride nuclei yields the contribution to the relaxation of HT11 resulting from dipole–dipole interactions with the other hydrides, $R_{H(m)H}$. $R_{H(m)H}$ was calculated for each of the five hydrides and these terms were averaged to yield the average hydride–hydride contribution to the hydride relaxation rate. The contributions to hydride relaxation from hydride–ortho hydrogen, and hydride–methyl hydrogen dipole–dipole interactions were calculated similarly (Table XI).

Contributions to hydride relaxation due to hydride–phosphorus dipole–dipole interactions were calculated by using eq 20, where r_{HP} is the P–H internuclear distance (Å). Again the interactions

$$R_{HP} = \frac{11.87\ \text{Å}^6\ \text{s}^{-1}}{(r_{HP})^6} \quad (20)$$

of a given hydride with all three phosphorus nuclei were summed to give the total relaxation rate, R_{HP}, for each hydride. These five terms were summed and divided by five to give the average contribution to hydride relaxation due to phosphorus–hydride dipole–dipole interactions (Table XII).

The contribution to hydride relaxation due to hydride–rhenium dipole–dipole interactions was calculated by using eq 21, where

$$R_{HRe} = 0.375\left(\frac{44.98\ \text{Å}^6\ \text{s}^{-1}}{(r_{HRe})^6}\right) + 0.625\left(\frac{45.88\ \text{Å}^6\ \text{s}^{-1}}{(r_{HRe})^6}\right) \quad (21)$$

the first term represents the relaxation arising from ^1H–^{185}Re interactions (37.5% natural abundance) and the second term represents the relaxation arising from ^1H–^{187}Re interactions (62.5% natural abundance). Again the relaxation rates, R_{HRe}, for each hydride were summed and divided by five to obtain the average rhenium–hydride contribution to relaxation (Table XII).

The calculated relaxation rate for the hydride ligands in $[ReH_5(PMePh_2)_3]$ is the sum of the contributions from all the nuclei, i.e., other hydrides, ortho hydrogens, methyl hydrogens, phosphorus, and rhenium (eq 22).

$$R_{cal} = R_{H(m)H} + R_{H(l)H}(\text{ortho}) + R_{H(l)H}(\text{Me}) + R_{HP} + R_{HRe} = 3.129\ \text{s}^{-1} + 1.125\ \text{s}^{-1} + 0.430\ \text{s}^{-1} + 0.090\ \text{s}^{-1} + 1.968\ \text{s}^{-1} = 6.742\ \text{s}^{-1} \quad (22)$$

Intrinsic Binding Properties of a Differentiated Iron Subsite in Analogues of Native $[Fe_4S_4]^{2+}$ Clusters

John A. Weigel and R. H. Holm*

Contribution from the Department of Chemistry, Harvard University, Cambridge, Massachusetts 02138-2902. *Received December 24, 1990*

Abstract: The cubane-type clusters $[Fe_4S_4(LS_3)L']^{z-}$ (**3**; LS_3 = 1,3,5-tris((4,6-dimethyl-3-mercaptophenyl)thio)-2,4,6-tris-(*p*-tolylthio)benzene(3–)) contain $[Fe_4S_4]^{2+}$ core units whose iron subsites are differentiated in the ratio 3:1. In the first extensive study of its kind, the intrinsic binding affinities at the unique subsite toward a large variety of biological and abiological ligands have been examined in Me_2SO solutions. The clusters $[Fe_4S_4(LS_3)Cl]^{2-}$ (**4**) and $[Fe_4S_4(LS_3)(OC_6H_4\text{-}p\text{-}Br)]^{2-}$ (**18**), which have been isolated, undergo subsite-specific, usually stoichiometric, substitution reactions with free ligands and trimethylsilyl reagents, respectively. A set of some 30 clusters of type **3** with four-, five-, and six-coordinate subsites have been generated in situ from **4** and **18**. These reactions can be monitored by ^1H NMR owing to the extreme sensitivity of ligand isotropic shifts to the identity of ligand L′ at the unique subsite. The ligands RS^-, RO^-, CN^-, and N_3^- afford four-coordinate subsites, while certain chelating ligands lead to five- and six-coordinate subsites. Among the clusters produced are those that simulate the binding of Tyr·O^-, Ser·O^-, Asp/Glu·CO_2^-, one or two Cys·S^-, and three His·Im protein side chain groups and the solvated and deprotonated (hydroxide) forms of native clusters. Ligand binding reactions are accompanied by changes in $[Fe_4S_4]^{2+/1+}$ redox potentials, which provide another means of detecting product clusters and convey the sign of the intrinsic potential shift upon variation of ligands at the unique subsite. These results are pertinent to the reaction chemistry of native subsite-differentiated clusters such as that in aconitase, which in the resting state exists with H_2O/OH^- at the unique subsite.

Introduction

The function of the all-cysteinate ligated cluster **1** as an electron transfer center in ferredoxin (Fd) proteins and in enzymes is widely recognized. However, it is now evident that electron transfer is not the sole biological function of Fe_4S_4 clusters. Among the most significant recent developments in iron–sulfur biochemistry is the recognition of a class of enzymes that contain Fe–S clusters and no other prosthetic groups and catalyze *nonredox* transformations. Of these, the only one for which interpretation of active site structure and reaction pathway has been reduced to a molecular level is aconitase.[1,2] This enzyme is an isomerase, catalyzing the

(1) Beinert, H.; Kennedy, M. C. *Eur. J. Biochem.* **1989**, *186*, 5.

0002-7863/91/1513-4184$02.50/0

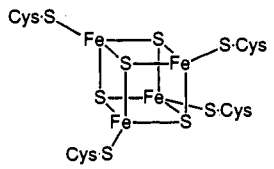

1

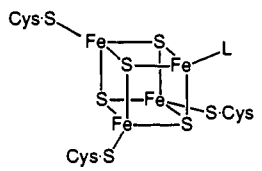

2

interconversion of citrate and isocitrate at an Fe_4S_4 cubane-type cluster catalytic site.[1-3] This cluster has been characterized crystallographically in the resting enzyme as the subsite-differentiated species **2** with L = H_2O or OH^-.[4] Indeed, it is one of only three cases in which the generalized cluster **2** has been recognized. In the 8-Fe form of *Desulfovibrio africanus Fd* III, one of the two Fe_4S_4 clusters has a non-cysteinate ligand,[5a] as does the single Fe_4S_4 cluster in *Pyrococcus furiosus Fd*.[5b] On the basis of amino acid sequences, ligand L could be Asp·CO_2^- and/or water or hydroxide. The biological functions of these proteins are unknown.

Substrate binding and catalysis in aconitase is one example of what we have termed "subsite-specific" properties of native Fe_4S_4 clusters. Elsewhere we have summarized subsite-specific structural and reactivity properties of these clusters.[6] In order to contribute to an understanding of these properties, we have developed the clusters $[Fe_4S_4(LS_3)L']^{z-}$ of structure **3**,[7-11] in which the Fe_4S_4

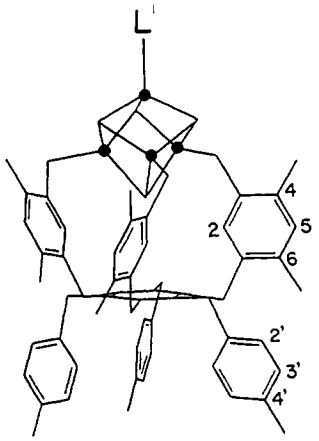

3 (● = Fe)

core is bound by the semirigid tridentate cavitand ligand LS_3,[10] resulting in a 3:1 differentiation of iron subsites. We have demonstrated certain substitution reactions at the unique subsite that have afforded four-,[7-10] five-,[9] and six-coordinate[9,11] subsites, with attendant structural and electronic influences on core properties.

It is now apparent that aconitase is not an isolated case of a nonredox enzyme that utilizes an Fe_4S_4 cluster as the catalytic site.[2] Other examples include a dehydratase,[12] an endonuclease,[13] and an amidotransferase.[14] In another dehydratase, an Fe_2S_2 cluster appears to play a related role.[15] Collective Mössbauer[16] and ENDOR[17-19] spectroscopic results for aconitase make it certain that the unique iron subsite is the locus of substrate and inhibitor binding. By implication, the less well characterized enzymes may contain a type **2** cluster with one subsite differentiated by a ligand that would be easily displaced by substrate, an unlikely aspect of cysteinate binding. These matters raise the question of the intrinsic ligand affinity and reactivity of an iron subsite in an Fe_4S_4 cluster, especially in the $[Fe_4S_4]^{2+}$ oxidation state of the foregoing enzyme clusters. We present here an examination of the subsite-specific reactivity properties of the clusters **3** with a variety of ligands introduced by two types of substitution reactions. This work considerably expands our previous information on subsite reactivity and possible modes of non-cysteinate ligation to synthetic and protein-bound clusters.

Experimental Section

Preparation of Compounds. All operations were carried out under a pure dinitrogen atmosphere. Acetonitrile was distilled from CaH_2 and THF from sodium benzophenone ketyl. Me_2SO and other deuterated solvents were dried over molecular sieves prior to use. $(Ph_4P)_2[Fe_4S_4(LS_3)Cl]$[7] (**4**), $Li_3[VS_4]\cdot 2DMF$,[20] and PhTeTePh[21] were prepared by published methods. All other compounds were commercial samples and were used as received. Sodium phenolates and thiolates were obtained by the reaction of NaH with the phenol or thiol in THF. The compounds LiSePh, LiTePh, and Li_2Se were prepared by the reaction of PhSeSePh, PhTeTePh, and selenium shot, respectively, with $LiEt_3BH$ in THF.

$(Ph_4P)_2[Fe_4S_4(LS_3)(OC_6H_4$-*p*-Br)] (**18**). A solution of 25.4 mg (0.130 mmol) of $NaOC_6H_4$-*p*-Br in 1 mL of acetonitrile was added to a solution of 250 mg (0.124 mmol) of **4** in 10 mL of acetonitrile. The reaction mixture was stirred for 1 h and filtered through Celite. Addition of 40 mL of ether to the filtrate and storage at −20 °C overnight resulted in the separation of a dark red-brown solid. This material was collected by filtration, washed with ether, and dried in vacuo to afford 160 mg (60%) of product pure by ^1H NMR. ^1H NMR (anion, Me_2SO): δ 2.22 (4′-Me), 3.74 (4-Me), 3.95 (6-Me), 4.54 (2-H), 6.74 (3′-H), 7.20 (2′-H), 8.24 (5-H), 8.93 (*m*-H).

Generation of Clusters in Solution. A series of clusters $[Fe_4S_4(LS_3)L']^{z-}$ was prepared in situ by chloride substitution of **4** by ligands L'^{z-} and by the reaction of trimethylsilyl reagents with **18**. In a typical experiment, a known amount of reagent M^IL', L′, or Me_3SiL' (usually 1.05–1.10 equiv) as a solution in Me_2SO-d_6 was added via syringe to a ca. 5 mM solution of **4** or **18** in Me_2SO-d_6. Reactions were immediate. The reagents are indicated in Figures 1 and 2, and most are listed in the following section. Product identity was established by ^1H NMR spectroscopy, and redox potentials were determined by cyclic voltammetry.

Physical Measurements. All measurements were performed under strictly anaerobic conditions. ^1H NMR spectra were measured on a Brüker AM-500 spectrometer. Electrochemical measurements were performed in Me_2SO solutions by using standard PAR instrumentation, a Pt working electrode, a SCE reference electrode, and 0.1 M $LiClO_4$ or 0.1 M $(Bu_4N)(PF_6)$ supporting electrolyte. Under the experimental conditions, $E_{1/2}(Fc^+/Fc)$ = 0.46 V.

The clusters $[Fe_4S_4(LS_3)L']^{z-}$ are detected by their ^1H isotropic shifts, which are collected in Table I. Salts of the ligands in Me_2SO were taken

(2) Emptage, M. H. *Metal Clusters in Proteins*; Que, L., Jr., Ed.; ACS Symposium Series 372; American Chemical Society: Washington, DC, 1988; Chapter 17.
(3) (a) Kennedy, M. C.; Emptage, M. H.; Dreyer, J.-L.; Beinert, H. *J. Biol. Chem.* **1983**, *258*, 11098. (b) Emptage, M. H.; Dreyer, J.-L.; Kennedy, M. C.; Beinert, H. *J. Biol. Chem.* **1983**, *258*, 11106.
(4) (a) Stout, C. D. *Proc. Natl. Acad. Sci. U.S.A.* **1989**, *86*, 3639; *Proteins* **1989**, *5*, 289.
(5) (a) George, S. J.; Armstrong, F. A.; Hatchikian, E. C.; Thomson, A. J. *Biochem. J.* **1989**, *264*, 275. (b) Conover, R. C.; Kowal, A. T.; Fu, W.; Park, J.-B.; Aono, S.; Adams, M. W. W.; Johnson, M. K. *J. Biol. Chem.* **1990**, *265*, 8533.
(6) Holm, R. H.; Ciurli, S.; Weigel, J. A. *Prog. Inorg. Chem.* **1990**, *38*, 1.
(7) Stack, T. D. P.; Holm, R. H. *J. Am. Chem. Soc.* **1988**, *110*, 2484.
(8) Stack, T. D. P.; Carney, M. J.; Holm, R. H. *J. Am. Chem. Soc.* **1989**, *111*, 1670.
(9) Ciurli, S.; Carrié, M.; Weigel, J. A.; Carney, M. J.; Stack, T. D. P.; Papaefthymiou, G. C.; Holm, R. H. *J. Am. Chem. Soc.* **1990**, *112*, 2654.
(10) Stack, T. D. P.; Weigel, J. A.; Holm, R. H. *Inorg. Chem.* **1990**, *29*, 3745. LS_3 = 1,3,5-tris((4,6-dimethyl-3-mercaptophenyl)thio)-2,4,6-tris(*p*-tolylthio)benzene(3−).
(11) Weigel, J. A.; Srivastava, K. K. P.; Day, E. P.; Münck, E.; Holm, R. H. *J. Am. Chem. Soc.* **1990**, *112*, 8015.
(12) Kuchta, R. D.; Hanson, G. R.; Holmquist, B.; Abeles, R. H. *Biochemistry* **1986**, *25*, 7301.
(13) Cunningham, R. P.; Asahara, H.; Bank, J. F.; Scholes, C. P.; Salerno, J. C.; Surerus, K. K.; Münck, E.; McCracken, J.; Peisach, J.; Emptage, M. H. *Biochemistry* **1989**, *28*, 4450.
(14) (a) Grandoni, J. A.; Switzer, R. L.; Makaroff, C. A.; Zalkin, H. *J. Biol. Chem.* **1989**, *264*, 6058. (b) Vollmer, S. J.; Switzer, R. L.; Debrunner, P. G. *J. Biol. Chem.* **1983**, *258*, 14284.
(15) Flint, D. H.; Emptage, M. H. *J. Biol. Chem.* **1988**, *263*, 3558.
(16) (a) Emptage, M. H.; Kent, T. A.; Kennedy, M. C.; Beinert, H.; Münck, E. *Proc. Natl. Acad. Sci. U.S.A.* **1983**, *80*, 4674. (b) Kent, T. A.; Emptage, M. H.; Merkle, H.; Kennedy, M. C.; Beinert, H.; Münck, E. *J. Biol. Chem.* **1985**, *260*, 6871.
(17) (a) Telser, J.; Emptage, M. H.; Merkle, H.; Kennedy, M. C.; Beinert, H.; Hoffman, B. M. *J. Biol. Chem.* **1986**, *261*, 4840. (b) Kennedy, M. C.; Werst, M.; Telser, J.; Emptage, M. H.; Beinert, H.; Hoffman, B. M. *Proc. Natl. Acad. Sci. U.S.A.* **1987**, *84*, 8854.
(18) Werst, M. M.; Kennedy, M. C.; Beinert, H.; Hoffman, B. M. *Biochemistry* **1990**, *29*, 10526.
(19) Werst, M. M.; Kennedy, M. C.; Houseman, A. L. P.; Beinert, H.; Hoffman, B. M. *Biochemistry* **1990**, *29*, 10533.
(20) Zhang, Y.; Holm, R. H. *Inorg. Chem.* **1988**, *27*, 3875.
(21) Haller, W. S.; Irgolic, K. J. *J. Organomet. Chem.* **1972**, *38*, 97.

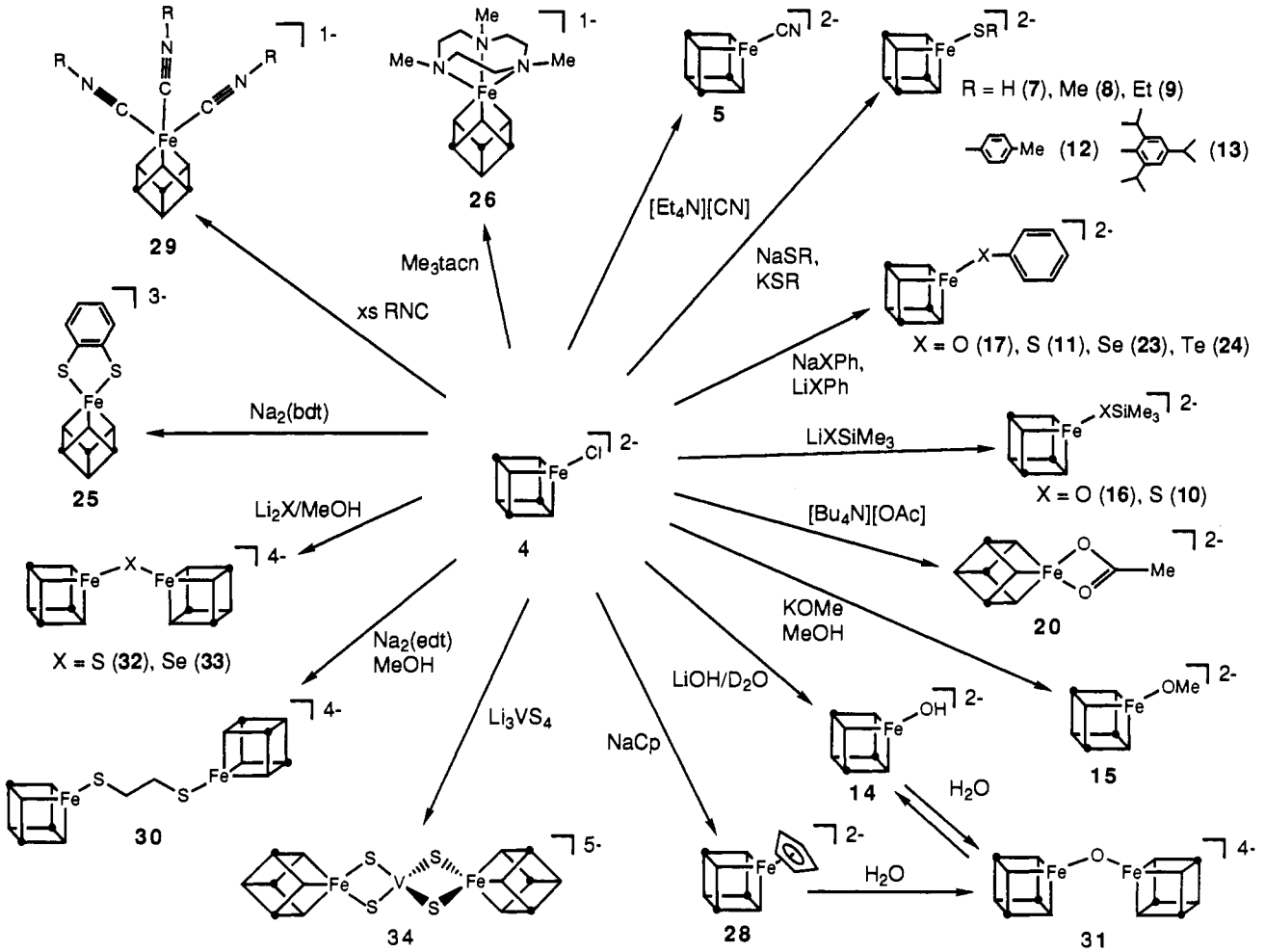

Figure 1. Summary of the subsite-specific substitution reactions of $[Fe_4S_4(LS_3)Cl]^{2-}$ (**4**) in Me_2SO solution effected by reaction with ligands L'^{z-} and L′ (**26**, **29**). Reagents were added in Me_2SO solutions unless otherwise indicated. In this and the next figure, the cube symbol represents the $Fe_4S_4(LS_3)$ cluster portion of **3**.

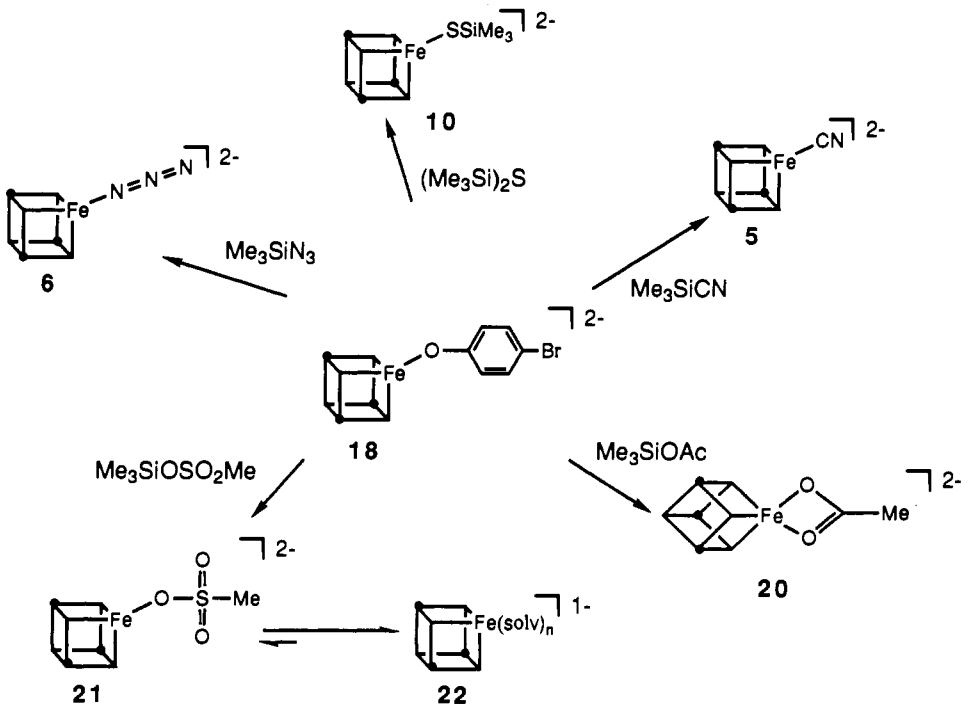

Figure 2. Summary of the subsite-specific reactions of $[Fe_4S_4(LS_3)(OC_6H_4\text{-}p\text{-}Br)]^{2-}$ (**18**) in Me_2SO solution effected by reaction with Me_3SiL' reagents; solv = MeCN, Me_2SO.

Table I. ^1H Isotropic Shifts and Redox Potentials of $[Fe_4S_4(LS_3)L']^{z-}$ Clusters in Me_2SO at 297 K

		$(\Delta H/H_0)_{iso}$,[a] ppm				
no.	L′	4-Me	5-H	6-Me	L′[b]	$E_{1/2}$,[c] V
4	Cl–	−1.96	−1.42	−1.84		−0.86
5	CN–	−2.00	−1.31	−1.77		−0.84
6	N_3–	−1.98	−1.43	−1.86		−0.91[o]
7	HS–	−1.83	−1.35	−1.79		−1.01
8	MeS–	−1.76	−1.33	−1.78	−13.46	−1.04
9	EtS–	−1.75	−1.32	−1.78	−10.85 (CH_2), −1.28 (Me)	−1.08
10	Me_3SiS–	−1.78	−1.35	−1.81	−0.86	−1.04
11	PhS–	−1.83	−1.34	−1.80	1.27, −1.45, 1.22	−0.97
12	*p*-MeC_6H_4S–	−1.82	−1.35	−1.82	1.14, −1.69, −1.87	−0.99
13	2,4,6-$iPr_3C_6H_2S$–	−1.75	−1.32	−1.78	−0.43, (Me), 1.12 (CH), −1.56, −0.06 (Me)[d]	−1.03
14	HO–	−1.96	−1.42	−1.84		−1.05
15	MeO–	−1.80	−1.40	−1.86	*n*	−1.08
16	Me_3SiO–	−1.82	−1.44	−1.90	−0.64	−1.09
17	PhO–	−1.90	−1.45	−1.91	*e*, −2.20, 1.56	−0.99
18	*p*-BrC_6H_4O–	−1.92	−1.45	−1.90	*e*, −2.18	−0.98
19	*p*-MeC_6H_4O–	−1.89	−1.44	−1.90	*e*, −2.30, −2.68	−1.01
20	OAc–	−1.95	−1.42	−1.85	−3.10	−0.95[o]
22	$(MeCN)_n$[f]	−2.21	−1.49	−1.86		−0.72[o]
23	PhSe–	−1.79	−1.32	−1.78	*e*, −1.44, 0.78	*g*
24	PhTe–	−1.72	−1.28	−1.73	*e*, −1.45, 0.45	*g*
25	$[1,2\text{-}C_6H_4S_2]^{2-}$[h]	−1.65	−1.54	−2.02	−1.05 (4,5-H), −2.89 (3,6-H)	−1.38
26	Me_3tacn	−2.15	−1.78	−2.28	−5.11, −7.44 (CH)	−1.09
27	$[HBpz_3]^{1-}$[h]	−2.15	−1.87	−2.36		−1.40[i]
28	C_5H_5–	−1.87	−1.60	−2.04	13.1	*j*
29	$(t\text{-}BuNC)_3$[k]	−9.09	−9.65	−12.98	1.14	−0.98
30	$[1,2\text{-}C_2H_4S_2]^{2-}$[l]	−1.77	−1.30	−1.79	−10.55	−1.13, −1.20[m]
31	O^{2-}	−2.32	−2.05	−2.73		−1.24, −1.47
32	S^{2-}	−2.15	−1.82	−2.49		−1.17, −1.39
33	Se^{2-}	−1.98	−1.69	−2.36		−1.17, −1.40
34	VS_4^{3-}	−2.21	−1.96	−2.41		−1.05, −1.13

[a] $(\Delta H/H_0)_{iso} = (\Delta H/H_0)_{dia} - (\Delta H/H_0)_{obs}$. [b] For aryl ligands, shifts are given in the order ortho, meta, para. [c] Vs SCE; ν = 50 mV/s, $[Fe_4S_4]^{2+/1+}$ couple. [d] *p*-CH not observed. [e] *o*-H not observed. [f] Acetonitrile solution. [g] Not determined. [h] Reference 9. [i] Dichloromethane. [j] Too unstable for measurement. [k] Reference 11. [l] Reference 8. [m] DMF. [n] Me not observed. [o] 0.1 M $(Bu_4N)(PF_6)$ supporting electrolyte.

as diamagnetic references; chemical shifts of Na_3LS_3 are given elsewhere.[9] Other reference shifts (ppm) are the following: NaCp, 5.31; KSMe, 1.68; NaSEt, 1.05 (t, Me), 2.21 (q, CH_2); $NaSSiMe_3$, −0.08; NaSPh, 6.10 (d, *o*-H), 6.43 (t, *p*-H), 6.68 (t, *m*-H); $NaSC_6H_2$-2,4,6-iPr_3, 1.02 (d, 2,6-Me), 1.10 (d, 4-Me), 2.62 (m, 4-CH), 4.22 (m, 2,6-CH), 6.50 (*m*-H); KOMe, 3.15; $LiOSiMe_3$, −0.27; NaOPh, 5.88 (t, *p*-H), 6.10 (d, *o*-H), 6.71 (t, *m*-H); $NaOC_6H_4$-*p*-Me, 1.98 (Me), 5.90 (d, *o*-H), 6.47 (d, *m*-H); $(Et_4N)(SC_6H_4$-*p*-Me), 2.03 (Me), 6.45 (d, *m*-H), 6.86 (d, *o*-H); $NaOC_6H_4$-*p*-Br, 6.00 (d, *o*-H), 6.75 (d, *m*-H); $(Bu_4N)(OAc)$, 1.52; LiSePh, 6.56 (t, *p*-H), 6.60 (t, *m*-H), 7.27 (d, *o*-H); LiTePh, 6.54 (t, *m*-H), 6.74 (t, *p*-H), 7.62 (d, *o*-H); Me_3tacn, 2.26 (Me), 2.60 (CH_2).

Results and Discussion

The clusters **3** are synthetic analogues of the subsite-differentiated biological cluster **2** such as has been proven in aconitase.[4] The subsite-specific reactivity of **3** has been examined in Me_2SO solutions with a variety of biological and abiological ligands. Product clusters were not isolated, but their formation was proven by differences in ^1H NMR spectra and in most instances by small changes in redox potentials determined by cyclic voltammetry. In each reaction system, addition of 0.5 equiv of reagent L'^{z-} or Me_3SiL' produced a spectrum consisting of 50% of the initial cluster and 50% of the product cluster, thereby identifying the latter. With one exception, the $[Fe_4S_4]^{2+}$ cores of all clusters **3** have an $S = 0$ ground state and excited paramagnetic states whose population affords isotropic shifts that are dominantly contact in origin.[22] The exquisite sensitivity of ^1H NMR chemical shifts to the identity of L′ in **3** and the narrow line widths, which render shifts determined at 297 K and 500 MHz precise to ±0.01 ppm, have been indispensable to the detection of reactivity. Certain examples of the use of this effect in demonstrating ligand substitution reactions of **3** have been presented earlier.[7-9] All clusters exhibit chemically reversible $[Fe_4S_4]^{2+/1+}$ redox couples, whose $E_{1/2}$ values could be determined with a precision of ±10 mV at the scan rate ν = 50 mV/s.

Reaction Systems. The solvent was chosen to be Me_2SO because of favorable solubility properties of reactants and products. Two reaction types were utilized to examine subsite-specific substitution reactions. One consists of the chloride substitution reactions 1 of cluster **4**. In other cases, sometimes involving weakly coordinating ligands, the reactions 2 of the *p*-bromophenolate cluster **18** with trimethylsilyl compounds were explored.

$$[Fe_4S_4(LS_3)Cl]^{2-} + L'^{z-} \rightarrow [Fe_4S_4(LS_3)L']^{(z+1)-} + Cl^- \quad (1)$$

$$[Fe_4S_4(LS_3)(OC_6H_4\text{-}p\text{-}Br)]^{2-} + Me_3SiL' \rightarrow [Fe_4S_4(LS_3)L']^{2-} + Me_3SiOC_6H_4\text{-}p\text{-}Br \quad (2)$$

Reaction 1 implies direct displacement of chloride by added ligand. Nearly all previous examples of this reaction were conducted in acetonitrile solution,[7-9,11] in which, given the relatively weak coordinating power of the solvent, dissociation of chloride is not expected. Evidence pertinent to the binding of chloride by cluster **4** in the more strongly coordinating medium provided by Me_2SO was acquired from the cyclic voltammetric results in Figure 3. These support the reaction scheme 3–6 ($n \leq 3$).

$$[Fe_4S_4(LS_3)Cl]^{2-} + e^- \overset{E_1}{\rightleftharpoons} [Fe_4S_4(LS_3)Cl]^{3-} \quad (3)$$

$$[Fe_4S_4(LS_3)Cl]^{3-} \xrightarrow{Me_2SO} [Fe_4S_4(LS_3)(Me_2SO)_n]^{2-} + Cl^- \quad (4)$$

$$[Fe_4S_4(LS_3)(Me_2SO)_n]^{2-} \overset{E_2}{\rightleftharpoons} [Fe_4S_4(LS_3)(Me_2SO)_n]^{1-} + e^- \quad (5)$$

$$[Fe_4S_4(LS_3)(Me_2SO)_n]^{1-} + Cl^- \rightarrow [Fe_4S_4(LS_3)Cl]^{2-} + nMe_2SO \quad (6)$$

The first three steps correspond to the $E_rC_iE_r$ coupled reaction case where $E_1 < E_2$.[23] Thus, upon the initial cathodic scan, **4**

(22) (a) Holm, R. H.; Phillips, W. D.; Averill, B. A.; Mayerle, J. J.; Herskovitz, T. *J. Am. Chem. Soc.* **1974**, *96*, 2109. (b) Reynolds, J. G.; Laskowski, E. J.; Holm, R. H. *J. Am. Chem. Soc.* **1978**, *100*, 5315.

(23) Brown, E. R.; Large, R. F. In *Physical Methods of Chemistry*; Weissberger, A., Rossiter, B. W., Ed.; Wiley-Interscience: New York, 1973; Vol. I, Part IIA, Chapter VI.

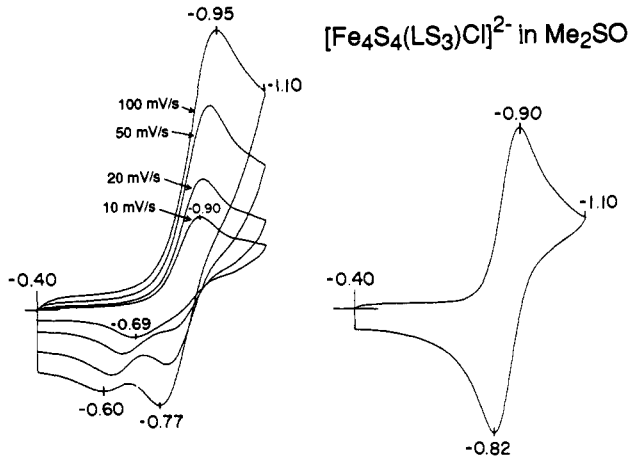

Figure 3. Cyclic voltammetry of $[Fe_4S_4(LS_3)Cl]^{2-}$ (**4**) in Me_2SO solution at 297 K; peak potentials vs SCE are indicated: left, voltammograms at ν = 10–100 mV/s in the presence of 0.1 M $LiClO_4$; right, voltammogram at ν = 50 mV/s in the presence of 0.1 M Et_4NCl.

is reduced to the trianion by the reversible electron transfer reaction 3; at scan rate ν = 100 mV/s, E_{pc} = −0.95 V. This is followed by irreversible loss of chloride and formation of a reduced solvated cluster in reaction 4. The anodic scan reveals two processes, at E_{pa} = −0.77 V and −0.60 V (100 mV/s), which correspond to the reverse of reaction 3 and to reaction 5, respectively. On the subsequent cathodic scan, the reduction of $[Fe_4S_4(LS_3)(Me_2SO)_n]^{1-}$ is not detected, presumably because of the irreversible reaction 6, which reforms starting cluster **4**.

The current function $i_p/\nu^{1/2}$ shows the behavior expected for the $E_rC_iE_r$ mechanism. For example, the function decreases by about 20% for the initial cathodic wave on increasing ν from 10 to 100 mV/s. The current ratio i_p^a/i_p^c of the more cathodic wave approaches unity as the scan rate is increased, as is expected because less time is allowed for chemical reaction 4 to occur. Note that the foregoing experiments were carried out in the presence of 0.1 M $LiClO_4$ supporting electrolyte. In the presence of 0.1 M Et_4NCl, the redox reaction of cluster **4** is effectively reversible with ΔE_p = 80 mV, i_p^a/i_p^c = 1, and $E_{1/2}$ = −0.86 V. Excess chloride suppresses reaction 4 and supports the argument that the species with E_{pc} = −0.60 V is the solvated cluster. We conclude that the reduced cluster $[Fe_4S_4(LS_3)Cl]^{3-}$, having the less positive core, irreversibly loses chloride in Me_2SO solution. In view of the solvated nature of the unique subsite in aconitase, reactions of a solvated oxidized cluster would be of interest. However, *oxidized* cluster **4** is largely or completely intact in this medium, and reaction 1, without mechanistic implication, is an appropriate statement of the substitution reactions. As will become evident, the other precursor cluster **18** and all other clusters except **21** are also intact in Me_2SO.

Subsite-Specific Reactions. The results of the reactions 1 and 2 are presented schematically in Figures 1 and 2, respectively. ^1H NMR isotropic shifts and redox potentials of some 30 clusters, including several from previous work, are collected in Table I. Here the clusters are arranged according to ligand type. Note that, in the generalized cluster **3**, three coordinating "arms" bind the cluster and are buttressed into position prior to cluster capture[10] by the three *p*-tolylthio "legs". While all signals of the arms and legs usually respond to changes in ligand L′, the isotropic shifts of 4-Me, 5-H, and 6-Me are generally the most sensitive and for that reason are included in Table I.

Reaction 1 addresses the matter of binding affinities of other ligands vs that of chloride. Reaction 2 provides another means of substitution, including the introduction of ligands that do not displace chloride, by taking advantage of the formation of the Si–O bond.[24] All reactions proceed to completion with 1.0–1.1 equiv of reactant, unless otherwise noted.[25]

(24) The dissociation energy of this bond in Me_3SiOH is reported to be 128 kcal/mol: Walsh, R. *Acc. Chem. Res.* **1981**, *14*, 246.

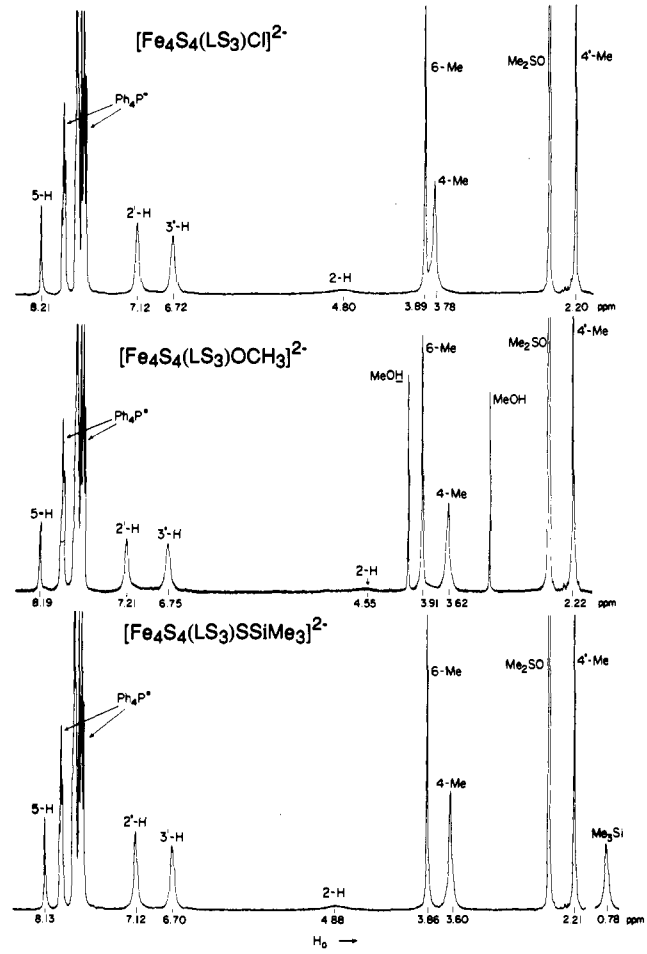

Figure 4. ^1H NMR spectra of initial cluster **4** in Me_2SO solution (top) and two of its substitution products, **15** (middle) and **10** (bottom), formed in situ in Me_2SO solutions by the reactions in Figure 1. In this and subsequent spectra, chemical shifts and signal assignments are indicated. Methanol appears in the spectrum of **15** because KOMe was added in a MeOH-d_4 solution. Paramagnetic and exchange broadening of the coordinated methoxide resonance presumably account for the failure to detect it in the spectrum.

(a) Monodentate Ligands. The ^1H NMR spectra of precursor cluster **4** is presented in Figure 4. The reaction of **4** with cyanide provides an example of the small changes in isotropic shift that allow detection of the product cluster, in this case **5** (Table I), for which the 5-H and 6-Me signals differ most from that of the initial cluster. The formation of **5** in dichloromethane solution is indicated by ν_{CN} = 2033 cm^{-1} compared to 2054 cm^{-1} for $(Et_4N)(CN)$ in this solvent. The detection by ^1H NMR of two other clusters formed in reaction 1 is illustrated in Figure 4. Binding of Me_3SiS^- to give **10** causes a shift of the 5-H resonance from 8.21 to 8.13 ppm and an upfield shift of the 4-Me signal by 0.18 ppm. These are the two largest changes, and an upfield shift of 5-H is always found upon binding monoanionic sulfur ligands. Reaction with excess methoxide to form **15** primarily influences the 2-H and 4-Me signals, which are displaced upfield by 0.25 and 0.16 ppm, respectively. While the 2-H signal, arising from a proton next to the C–S bond to the cluster, is sensitive to ligand changes, its large line width due to paramagnetic relaxation restricts its value in detecting ligand binding. Note that the spectra in Figure 4, as all other spectra of type **3** clusters determined in

(25) Excess quantities (ca. 3 equiv) of $LiOSiMe_3$, KOMe, and LiOH were required owing to the reaction of the anions with Ph_4P^+. These reactions presumably proceed in the manner of the decomposition of phosphonium hydroxides[26] to afford Ph_3PO and C_6H_6, which we have detected by NMR in several reaction systems.

(26) Hays, H. R.; Peterson, D. J. In *Organic Phosphorus Compounds*; Kosolapoff, G. M., Maier, L., Ed.; Wiley-Interscience: New York, 1972; Vol. 3, Chapter 6.

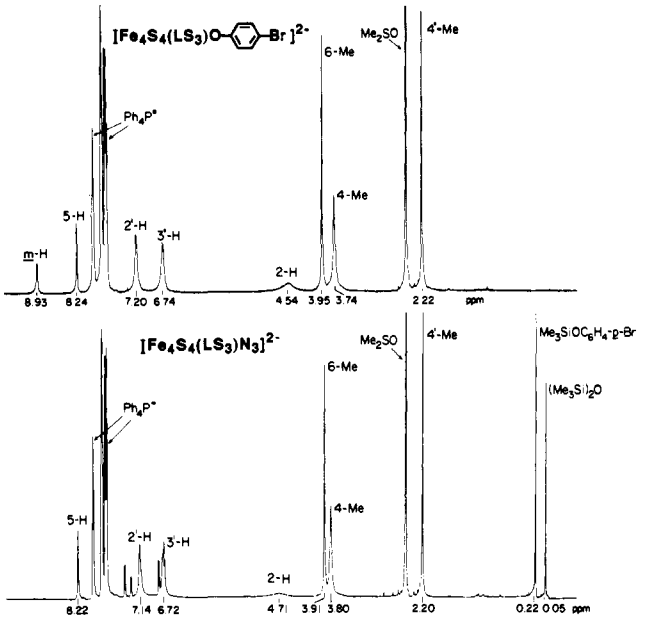

Figure 5. ^1H NMR spectra of initial cluster **18** in Me_2SO solution (upper) and one of its substitution products, **6** (lower), formed in situ in Me_2SO solution by the reaction in Figure 2.

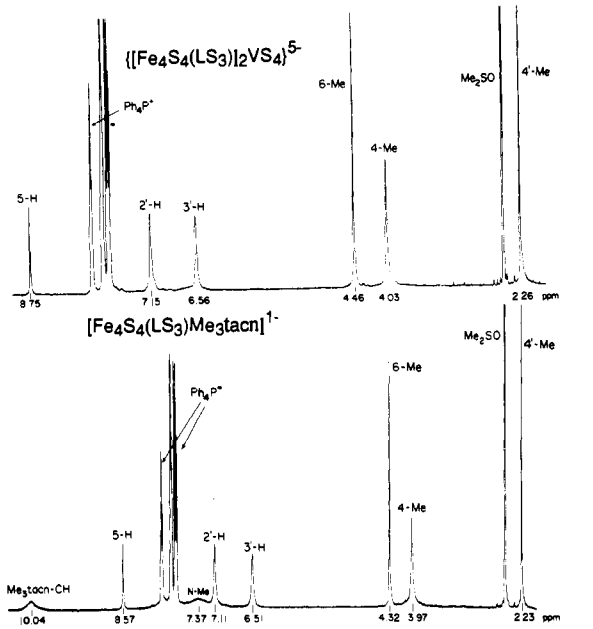

Figure 6. ^1H NMR spectra of bridged double cubane cluster **34** (upper) and cluster **26** (lower) containing a six-coordinate subsite, formed in situ in Me_2SO solutions by the reactions in Figure 1.

this and previous work, are consistent with effective trigonal symmetry.

Cluster **18** is readily obtained from **4** by ligand substitution. The *p*-bromophenyl group was found to facilitate isolation of an oxygen-ligated cluster required for reaction with trimethylsilyl reagents. The reaction of **18** with Me_3SiN_3 leads to the azide cluster **6**. Note that it and **4** are nearly indistinguishable by NMR, so the formation of **6** by chloride substitution could not have been detected by this criterion. The two clusters are, however, differentiated by a 50-mV difference in potentials, and the formation of **6** is further indicated by ν_{NNN} = 2064 cm^{-1} in acetonitrile solution.[27] The formation of **6** from **18** is readily determined by NMR, as illustrated in Figure 5 where it is seen that the phenolate *m*-H signal of **18** at 8.93 ppm is abolished upon reaction and resonances of the silyl ether product appear at 0.22 and near 7 ppm. The spectrum also contains the characteristic signal of $(Me_3Si)_2O$, which arises from hydrolysis of the silyl ether by trace water in the solvent. These observations also apply to the other reactions in Figure 2, among which is an alternative route to cyanide cluster **5**.

Cluster **4** reacts with a variety of anionic sulfur and oxygen ligands to afford the clusters **7–19**, which are depicted in Figure 1. Formation of sulfur-ligated clusters **7–13** is another expression of the high affinity of alkyl and arene thiolates for the subsites of the $[Fe_4S_4]^{2+}$ core. The binding of hydrosulfide in **7** is anticipated by the existence of $[Fe_4S_4(SH)_4]^{2-}$,[28] whose structure has been determined but whose other properties are uninvestigated. Cluster **10** is also available from the reaction of **18** and $(Me_3Si)_2S$ (Figure 2). The formation of **13** reveals that binding of a very bulky ligand is not impeded by the LS_3 ligand steric properties in solution, as suggested by solid-state structures.[7,10] The clusters $[Fe_4S_4(S\text{-}2,4,6\text{-}iPr_3C_6H_2)_4]^{2-,1-}$ have been prepared and are stable.[29]

With the apparent exception of **16**, oxygen-ligated clusters **14–19** are differentiated from their sulfur counterparts by larger isotropic shifts of both LS_3 and L′ protons.[30] As one example, the isotropic shifts of the pair **19**/**12** differ by the ratios 1.038 (4-Me), 1.067 (5-H), and 1.044 (6-Me). These ratios are substantially higher for L′ shifts, which are directly influenced by oxygen vs sulfur atom binding: 1.36 (*m*-H), 1.43 (*p*-Me). These latter observations are consistent with the isotropic shifts of the clusters $[Fe_4S_4(XAr)_4]^{2-}$, for which there are no exceptions to the shift order X = O[31] > S[22]). The alternating signs of the shifts of ring protons in **11**, **12**, and **17–19** and the reversal in sign in **12** and **19** when *p*-Me is substituted for *p*-H are consistent with dominant or exclusive contact interactions.

Other monodentate ligands that bind at the unique subsite in essentially stoichiometric reactions are benzeneselenolate and benzenetellurolate, which generate **23** and **24**, respectively (Figure 1). Of ligands of these types, only the binding of $PhSe^-$ to an Fe_4S_4 cluster, in $[Fe_4S_4(SePh)_4]^{2-}$,[32] has been previously demonstrated. To an extent, the binding of $PhTe^-$ is anticipated by this result and by the preparation of $[Fe_4Te_4(TePh)_4]^{3-}$.[33] Note that contact interactions continue to dominate the isotropic shifts of **23** and **24**.

(b) Bidentate and Tridentate Ligands. Treatment of **4** with a stoichiometric quantity of $(Bu_4N)(OAc)$ yielded a species whose NMR spectrum was nearly identical with that of **4**, except for the appearance of the acetate methyl resonance at 4.62 ppm (confirmed by deuteration). Identification of the product as acetate cluster **20** was further made on the basis of a change in redox potential to −0.93 V.[34]

We have shown earlier that a variety of bidentate ligands, including dithiocarbamate, pyridine-2-thiolate, bis(pyrazolyl)-hydroborate, and benzene-1,2-dithiolates, bind to the unique site in **3**.[9] One example of a species with a five-coordinate subsite,

(27) For $(Et_4N)N_3(MeCN)$ and $KN_3(KBr)$, ν_{NNN} = 2002 and 2041 cm^{-1}, respectively. An increase in ν_{NNN} over that of the uncoordinated ion is usual in metal(II,III) complexes: Nakamoto, K. *Infrared and Raman Spectra of Inorganic and Coordination Compounds*, 4th ed.; Wiley-Interscience: New York, 1986; pp 290–291.

(28) Müller, A.; Schladerbeck, N. H.; Bögge, H. *J. Chem. Soc., Chem. Commun.* **1987**, 35.

(29) O'Sullivan, T.; Millar, M. M. *J. Am. Chem. Soc.* **1985**, *107*, 4096.

(30) In the pair **16**/**10**, this generality holds for the LS_3 but not for the Me_3SiX^- (X = O, S) isotropic shifts. The shifts of these ligands, which appear in Table I, are calculated from the chemical shifts of Li^+ or Na^+ salts, which may not be the most appropriate diamagnetic references. However, use of the shifts of $(Me_3Si)_2X$ (both 0.05 ppm in Me_2SO) affords the same isotropic shift order: −0.32 ppm (**16**), −0.73 ppm (**10**).

(31) Cleland, W. E.; Holtman, D. A.; Ibers, J. A.; DeFotis, G. C.; Averill, B. A. *J. Am. Chem. Soc.* **1983**, *105*, 6021.

(32) Bobrik, M. A.; Laskowski, E. J.; Johnson, R. W.; Gillum, W. O.; Berg, J. M.; Hodgson, K. O.; Holm, R. H. *Inorg. Chem.* **1978**, *17*, 1402.

(33) Simon, W.; Wilk, A.; Krebs, B.; Henkel, G. *Angew Chem., Int. Ed. Engl.* **1987**, *26*, 1009.

(34) The FT IR spectrum of cluster **20** (acetonitrile solution) lacked the feature above 1600 cm^{-1} indicative of monodentate acetate, and any bands due to bidentate acetate at lower frequencies were obscured by ligand absorption. Thus, the bidentate structure of **20** in Figure 1 is assumed and not proven.

the benzene-1,2-dithiolate cluster **25**, is included in Table I and Figure 1. Detection of the bidentate functionality is made clear by comparison of isotropic shifts with those of benzenethiolate cluster **11** or any other monothiolate species. Decreased 4-H and increased 5-H and 6-Me shifts are characteristic of this class of clusters,[9] as are downfield-shifted phenylene protons and negatively shifted redox potentials. Reaction with the flexible ligand ethane-1,2-dithiolate, which usually functions in the chelate mode,[35] forms instead the bridged double cubane **30**.

The tridentate ligands 1,4,7-trimethyltriazacyclononane (Me_3tacn) and tris(pyrazolyl)hydroborate ($HB(pz)_3^-$) afford the clusters **26** and **27** (not shown), respectively. Their formation is revealed by significantly increased LS_3 isotropic shifts, as illustrated for **26** in Figure 6. Particularly evident is the shift of 5-H by 0.36 ppm downfield relative to **4**. The rigidity of these ligands argues for their tridentate function. When the unsubstituted ligand tacn is used, the formation of $[Fe_4S_4(LS_3)(tacn)]^{1-}$ is made apparent by the appearance of two tacn CH signals at 8.67 and 12.89 ppm. This observation is consistent with a six-coordinate subsite and rapid equilibration of inequivalent protons of individual methylene groups by interconversion of the gauche-type chelate ring conformations found for $[Fe(tacn)_2]^{2+,3+}$.[36] With **26** (Figure 6), the broad feature at 10.0 ppm is presumably a CH signal, the other broad CH and the N-Me resonances being at 7.37 ppm and obscured by the cation features near 8 ppm.

Reaction of **4** with NaCp yields a product with altered LS_3 shifts and an upfield resonance at −7.79 ppm. We assign this species as Cp cluster **28**. It is of limited stability and is extremely sensitive to protic impurities; we were unable to determine its redox potential. This is the first organometallic derivative of a biologically relevant Fe_4S_4 cluster. The cubane-type clusters $[Cp_4Fe_4S_4]^{0,1+,2+}$ had been prepared some time ago.[37-39]

Lastly, reaction of **4** with excess *t*-BuNC leads to the formation of **29** in a reversible equilibrium reaction. As shown elsewhere,[11] clusters of this type differ from all other $[Fe_4S_4]^{2+}$ clusters by having a paramagnetic ground state with attendant large isotropic shifts. The unique iron atom is rendered low-spin Fe^{II} by coordination of three isonitrile ligands, leaving an $[Fe_3S_4]^0$ cluster fragment with $S = 2$. The indicated coordination at the unique subsite has been proven by an X-ray structure determination.[11]

(c) Bridged Double Cubanes. Cluster **30** is one member of a set of double cubane clusters prepared by using suitable dithiolates in reaction 1.[8] Their formation may be detected by small shift changes and by coupled redox reactions if the separation of subclusters is not too great. A more intimately linked set of double cubanes **31**–**33** may be obtained by the reactions in Figure 1.

Reaction of **4** with excess LiOH or hydrolysis of Cp cluster **28** yields a mixture of two new species. One of these we identify as the hydroxide cluster **14** and the other as the μ-oxo-bridged double cubane **31**, mainly on the basis of the electrochemical results in Figure 7. Three peaks are observed in the differential pulse polarograms A–D. The two equally intense peaks at −1.24 and −1.47 V decrease and that at −1.05 V increases in intensity with increasing water content. Reactions 7 and 8 account for this

$$2[Fe_4S_4(LS_3)(Cp)]^{2-} + H_2O \rightarrow \{[Fe_4S_4(LS_3)]_2O\}^{4-} + 2CpH \quad (7)$$

$$\{[Fe_4S_4(LS_3)]_2O\}^{4-} + H_2O \rightarrow 2[Fe_4S_4(LS_3)(OH)]^{2-} \quad (8)$$

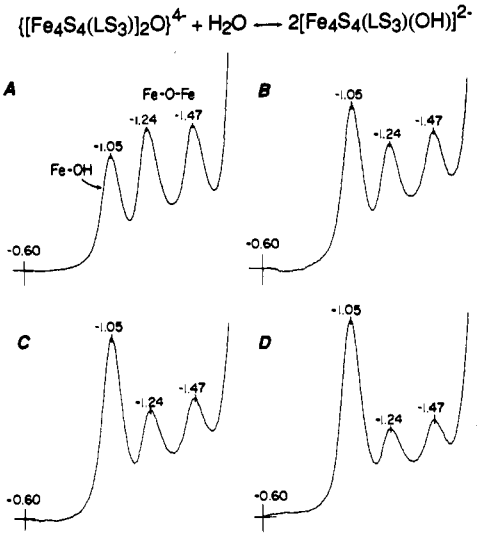

Figure 7. Differential pulse polarograms of cluster products obtained upon the reaction of ca. 1 mM **28** with water in Me_2SO solution: A, moist Me_2SO; B, 0.5% H_2O (v/v); C, 1% H_2O (v/v); D, 1.5% H_2O. Polarograms were recorded immediately after solution preparations; peak assignments (Fe–OH, **14**; Fe–O–Fe, **31**) and potentials vs SCE are indicated.

behavior, with the conversion of the μ-oxo double cubane to the hydroxide cluster being responsible for the changes in peak currents with water content. At 5% water (v/v), the peaks assigned to **31** are absent. Cluster **14** could not be identified by a substitution reaction of **4** with hydroxide inasmuch as the two have indistinguishable chemical shifts; however, their redox potentials differ by 190 mV. In the reaction system of Figure 7, the peak expected for **4** at or near −0.86 V is absent.

Treatment of **4** with 0.5 equiv of Li_2X affords the double cubanes with μ-sulfido (**32**) and μ-selenido (**33**) bridges. These are accompanied by minority amounts of single cubane **7** and its HSe^- analogue ($E_{1/2} = -1.01$ V), the protonated ligands arising from partial hydrolysis of X^{2-}. Both can be generated separately and identified by NMR and/or redox potential. The clusters **31**, **32**, and **33** form a series in which LS_3 isotropic shifts decrease in the order O > S > Se, a regularity that indirectly supports the bridged double cubane description. Within the groups of oxygen- and sulfur-ligated clusters having four-coordinate subsites, the shifts of **31** and **32**, respectively, are highly characteristic. Along the series, redox potentials and their differences ($\Delta E_{1/2}$ = 220–230 mV) are virtually constant. The μ-sulfido bridge has been structurally proven in $\{[Fe_4S_4Cl_3]_2S\}^{4-}$ (Fe–S–Fe = 102°, $\Delta E_{1/2}$ = 300 mV in acetonitrile)[40] and is probable in a $MoFe_3S_4$ double cubane.[41]

Other means of bridging cubane clusters are readily conceived, among them tetrathiometalate anions. The formation, from **4** and $[VS_4]^{3-}$, of double cubane **34**, whose NMR spectrum is given in Figure 6, is one example. The isotropic shifts are very different from those of **25**, which also has an FeS_5 subsite. The indicated chelate bridge structure is assumed by analogy with that for the linear cluster $[VFe_2S_4Cl_4]^{3-}$.[42] In this event, cluster **34**, as **25**, is fluxional at the unique subsite. The separation of 80 mV in redox potential is, from related work,[8] roughly consistent with an Fe···Fe subsite separation of ca. 6–7 Å. The Fe···Fe distance in $[VFe_2S_4Cl_4]^{3-}$ is 5.45 Å.

Redox Potentials. The redox reactions whose potentials are collected in Table I meet the cyclic voltammetry criterion of chemical reversibility ($i_{pc}/i_{pa} \approx 1$) but are not usually electrochemically reversible (ΔE_p = 59 mV, independent of ν).[23] All

(35) Rao, Ch. P.; Dorfman, J. R.; Holm, R. H. *Inorg. Chem.* **1986**, *25*, 428.
(36) Boeyens, J. C. A.; Forbes, A. G. S.; Hancock, R. D.; Wieghardt, K. *Inorg. Chem.* **1985**, *24*, 2926.
(37) (a) Schunn, R. A.; Fritchie, C. J., Jr.; Prewitt, C. T. *Inorg. Chem.* **1966**, *5*, 892. (b) Wei, C. H.; Wilkes, G. R.; Treichel, P. M.; Dahl, L. F. *Inorg. Chem.* **1966**, *5*, 900.
(38) (a) Trinh-Toan; Fehlhammer, W. P.; Dahl, L. F. *J. Am. Chem. Soc.* **1977**, *99*, 402. (b) Trinh-Toan; Teo, B. K.; Ferguson, J. A.; Meyer, T. J.; Dahl, L. F. *J. Am. Chem. Soc.* **1977**, *99*, 408.
(39) It is now well-recognized that isoelectronic members of the $[Cp_4Fe_4S_4]^z$ and $[Fe_4S_4(SR)_4]^z$ series are not electronically analogous, primarily because, in the latter, local metal sites are high-spin. For one discussion of this matter, cf. Chu, C. T.-W.; Dahl, L. F. *J. Am. Chem. Soc.* **1982**, *104*, 3409.
(40) Challen, P. R.; Koo, S.-M.; Dunham, W. R.; Coucouvanis, D. *J. Am. Chem. Soc.* **1990**, *112*, 2455.
(41) Challen, P. R.; Koo, S.-M.; Kim, C. G.; Dunham, W. R.; Coucouvanis, D. *J. Am. Chem. Soc.* **1990**, *112*, 8606.
(42) Do, Y.; Simhon, E. D.; Holm, R. H. *Inorg. Chem.* **1985**, *24*, 4635.

measurements of potentials were carried out in the presence of 0.1 M $LiClO_4$ supporting electrolyte, except for clusters **6**, **20**, and **21**. The potentials of these species, which contain particularly labile ligands subject to possible displacement by perchlorate, were determined in the presence of 0.1 M $(Bu_4N)(PF_6)$. The potential of −0.91 V for azide cluster **6** shifted to −0.88 V in the presence of 0.1 M $LiClO_4$. Acetate cluster **20** behaved similarly. We attribute the latter value to a species that is largely or completely ligated by perchlorate.

(a) Ligated Clusters. Earlier we had shown that stepwise ligand replacement of RS^- with Cl^- or OAc^- resulted in positive potential shifts of $[Fe_4S_4]^{2+/1+}$ couples.[43] While potential differences are often small, the more extensive body of data in Table I allows the recognition of this and other trends. The foregoing observation is further supported by, e.g., the 180-mV shift from **8** to **4** and the 90-mV shift from **8** to **20**. An additional regularity is that, at parity of R substituent, potentials for RO^- vs RS^- ligated clusters are more negative. This is supported by comparative data for some six cluster pairs that span differences of −20 mV (**11**/**17**, **12**/**19**) to −70 mV (**32**/**31**). Within these groups of clusters, potentials respond to substituent effects in the expected order; e.g., **7** > **8** > **9** and **11** > **12** > **13**.

Potentials of clusters with five- and six-coordinate subsites have been considered in some detail elsewhere.[9] Briefly, **25** is much more difficult to reduce than **11** because of coordination of a second thiolate sulfur atom, increasing the cluster charge to 3− and introducing more electron density into the $[Fe_4S_4]^{2+}$ core. In the case of **26**, the 1− cluster charge is compensated by electron donation from three tertiary amine nitrogen atoms, with the result that the potential is actually more negative than the majority of values in Table I. Cluster **27** has both a 2− negative charge and a six-coordinate subsite, resulting in the most negative potential in the set.

(b) Solvated Clusters. The reaction of **18** with Me_3SiOSO_2Me in acetonitrile solution proceeds to give a species stable for ca. 10 min.[44] The NMR spectrum recorded immediately after reaction showed removal of the phenolate ligand (as in the spectrum of **6**, Figure 5) and LS_3 shifts different from those of **18**. When the reaction is carried out in Me_2SO containing 0.1 M $(Bu_4N)(PF_6)$, the product has a stability similar to that in acetonitrile and a well-defined redox step with $E_{1/2}$ = −0.72 V, a value that remained unchanged in the presence of 0.1 M $NaOSO_2Me$. Further, for this step, E_{pa} = −0.63 V at ν = 50 mV/s, indistinguishable from E_{pa} = −0.62 V (Figure 3) at the same scan rate for a process assigned earlier to reaction 5. We conclude that, in both solvents, the product is largely or completely the solvated cluster **22** rather than the intact methanesulfonate cluster **21** (Figure 2). Redox potentials of the couples $[Fe_4S_4(LS_3)(solv)_n]^{1-/2-}$ are more positive than any other values in Table I, presumably because of the 1− charge of the oxidized form and the relatively weak donor ability of solvent molecules. These potentials are ca. 400 mV more positive than that of **26**, whose redox reaction involves the same cluster charges.

Systems with No Reaction. Having demonstrated that nearly 20 ligand types react with cluster **4** by chloride substitution, we complete our observations by listing those species that do not compete effectively with chloride for cluster binding in reaction 1. In 5 mM solutions of **4** in Me_2SO, up to 5 equiv of the following species do not react by the ^1H NMR criterion: 1,4,7-trithiacyclononane, $Me_2NCH_2CH_2NMe_2$, Et_3P, $(MeO)_3P$, imidazole, tetrahydrothiophene, CO, $[WS_4]^{2-}$, $[ReS_4]^-$, $LiOSO_2CF_3$, SCN^-, NO_2^-, HSO_3^-, and $NaOP(O)(OPh)_2$.

Summary. This work represents the first comprehensive examination of ligand binding to protein analogue Fe_4S_4 clusters. The following are the principal findings and conclusions of this investigation.

(1) Reactions at the differentiated subsites of chloride cluster **4** and phenolate cluster **18** with free ligands and trimethylsilyl reagents, respectively, afford a set of some 30 clusters of general type **3** containing, variously, biological and abiological ligands and four-, five-, and six-coordinate subsites.

(2) Nearly all reactions in (1) can be effectively monitored by ^1H NMR because of the pronounced sensitivity of isotropically shifted ligand resonances to the identity of ligand(s) at the unique subsite.

(3) Ligands that afford four-coordinate subsites are the anionic types CN^-, N_3^-, RS^-, and RO^-; these ligands in excess do not produce subsites of higher coordination number.

(4) Possible modes of protein binding to generalized native cluster **2** with a four-coordinate subsite have been simulated in the forms of L = Cys·S^- (**8**, **9**), Tyr·O^- (**17**, **19**), Ser·O^- (**15**), Asp/Glu·CO_2^- (**20**). Binding simulations of L = His·Im and Met·SMe have not been obtained. Clusters **25** and $[Fe_4S_4(LS_3)(HBpz_3)]^{2-}$ (**27**) approximate the binding of two Cys·S^- and three His·Im, respectively.

(5) Hydroxide cluster **14** represents the deprotonated form of a solvated aquo species as in aconitase, and double cubane **31** supports the viability of a μ-oxo bridge in proteins.

(6) The reactions in (1) are accompanied by (usually) small but detectable changes in $[Fe_4S_4]^{2+/1+}$ redox potentials, which provide another means for detection of product clusters and, relative to **8**/**9**, convey the sign of the intrinsic potential shift upon passing from native cluster **2** to **3**.

(7) Oxidized solvated cluster **22** can be generated in solution; it does not bind its accompanying anion. Although of limited stability, **22** offers the possibility of binding the substrates and inhibitors of an enzyme such as aconitase.

In ongoing research, we are utilizing the results obtained here to examine bound substrate reactivity and to develop new means of linking metal complexes and clusters to the Fe_4S_4 unit. Lastly, we have synthesized a second tridentate trithiolate ligand of different design than the LS_3 molecule that is capable of binding Fe_4S_4 clusters and supporting site-specific reactions.[45]

Acknowledgment. This research was supported by NIH Grant GM 28856.

(43) Johnson, R. W.; Holm, R. H. *J. Am. Chem. Soc.* **1978**, *100*, 5338.
(44) After this time, a black precipitate separates and free LS_3 resonances appear in the ^1H NMR spectrum.
(45) Whitener, M. A.; Peng, G.; Holm, R. H. *Inorg. Chem.*, in press.